inorganics

MDPI

Supplementary Materials

Testing the Efficacy of the Synthesis of Iron Antimony Sulfide Powders from Single Source Precursors

Fadiyah Makin [1], Dalal Alzahrani [2], Firoz Alam [3], Floriana Tuna [2], and David J. Lewis [1,*]

[1] Department of Materials, The University of Manchester, Oxford Road, Manchester M13 9PL, UK; fadiyah.makin@postgrad.manchester.ac.uk
[2] Photon Science Institute, The University of Manchester, Oxford Road, Manchester M13 9PL, UK; dalal.alzahrani@postgrad.manchester.ac.uk (D.A.); Floriana.Tuna@manchester.ac.uk (F.T.)
[3] Department of Chemistry, The University of Manchester, Oxford Road, Manchester M13 9PL, UK; firoz.alam@manchester.ac.uk
* Correspondence: david.lewis-4@manchester.ac.uk

Table S1. Composition used for the synthesis of $Sb_{2(1-x)}Fe_{2x}S_3$ system.

Mole fraction [Fe]/[Fe]+[Sb]	$Fe[S_2CNEt_2]_3$	$Sb[S_2CNEt_2]_3$
0	0 mmol	0.40 mmol
0.2	0.40 mmol	1.6 mmol
0.4	0.40 mmol	0.60 mmol
0.6	0.40 mmol	0.26mmol
0.8	0.40 mmol	0.10mmol
1	0.40 mmol	0 mmol

Binary systems: Sb_2S_3 and Fe_xS_y

The thermal decomposition of precursor **(1)** and **(2)** synthesised at temperature 300, 400, 425, 450 and 475 for 1h resulted in a black residue which was analysed by P-XRD. P-XRD patterns of the nanocrystals resulted from $Sb[S_2CN(Et_2)]_3$ **(1)** at 400, 425, 450 and 475 ˚C are illustrated in Figure S1. The analysis revealed that the crystalline phase produced corresponded to orthorhombic stibnite (Sb_2S_3, ICDD: 01-073-0393) with lattice parameters a = 11.313 Å, b = 3.833 Å, and c = 11.225 Å. As shown in Figure SI, the intensities of peaks were similar in all cases with a slight increase in some of the peaks upon increase in the growth temperature.

P-XRD patterns of the nanoparticles resulting from decomposition of $[Fe(S_2CN(Et)_2)_3]$ **(2)** at 300, 400, 450 and 475 ˚C are illustrated in Figure S2. The diffraction peaks corresponded to a hexagonal pyrrhotite iron sulfide ($Fe_{0.95}S_{1.05}$, ICDD 01-075-0600) with lattice parameters a = 3.4303 Å, b = 3.4303 Å, and c = 5.6802 Å with major diffraction peaks corresponding to (100), (101), (102), (110) planes. There were no significant differences in the intensities of peaks of all four samples.

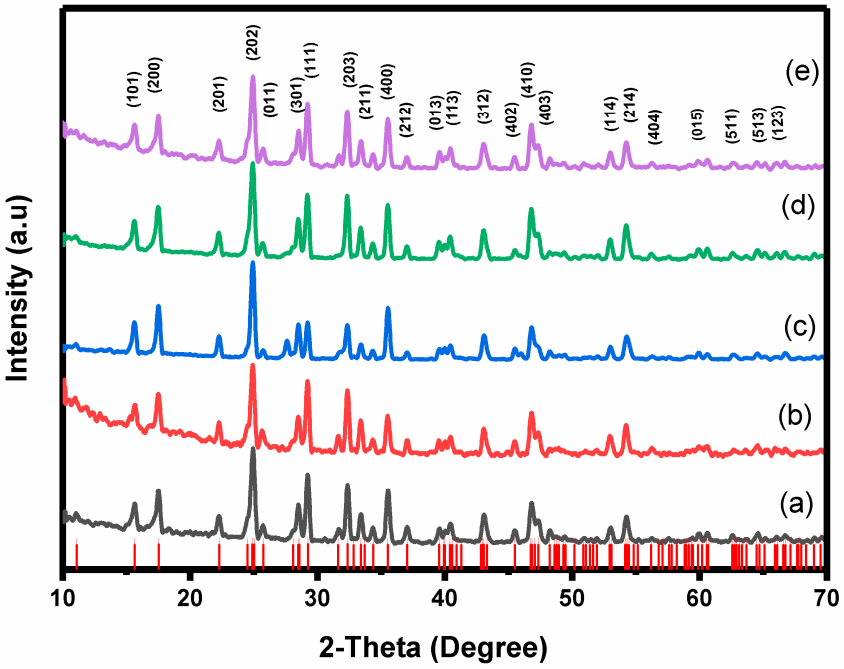

Figure S1. P-XRD patterns of Sb_2S_3 nanoparticles at (a) 300, (b) 400, (c) 425, (d) 450 and (e) 475 ˚C deposited from decomposition of $Sb(S_2CN(Et)_2)_3$ using melt method for 1h. All peaks corresponded to standard pattern of stibnite (ICDD 01-073-0393).

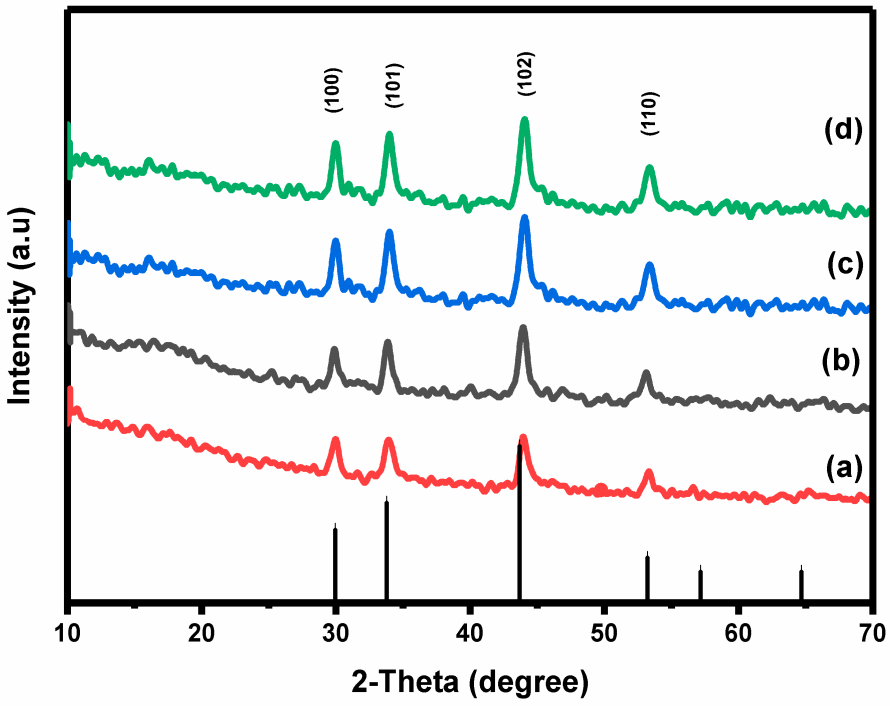

Figure S2. P-XRD patterns of FeS nanoparticles at (a) 300 ˚C, (b) 400 ˚C (c) 450 ˚C and (d) 475 ˚C from decomposition of $Fe(S_2CN(Et_2))_3$ using melt method for 1h. All peaks corresponded to standard pattern of pyrrhotite (ICDD 01-075-0600).

Table S2. The content of Fe, Sb and S in $Sb_{2(1-x)}Fe_{2x}S_3$ prepared by melt method at 450°C (x = 0, 0.2 , 0.4, 0.6, 0.8 and 1 molar fraction of iron) calculated from the feed rate and found by EDX measurement.

Mole Fraction	Elemental Composition Required (Atomic %)			Stoichiometry Required	Elemental Composition Found by EDX (atomic %)			Stoichiometry Found By EDX
	Fe	Sb	S		Fe	Sb	S	
0	0	40	60	Sb_2S_3	0	38.0	62.0	$Sb_{1.9}S_{3.1}$
0.2	8	32	60	$Fe_{0.4}Sb_{1.6}S_3$	9.1	32.7	58.2	$Fe_{0.4}Sb_{1.6}S_{2.9}$
0.4	16	24	60	$Fe_{0.8}Sb_{1.2}S_3$	17.9	26.9	55.2	$Fe_{0.8}Sb_{1.3}S_{2.75}$
0.6	24	16	60	$Fe_{1.2}Sb_{0.8}S_3$	23.5	18.9	57.9	$Fe_{1.15}Sb_{0.9}S_{2.85}$
0.8	32	8	60	$Fe_{1.6}Sb_{0.4}S_3$	32.98	21.76	45.27	$Fe_{1.6}Sb_{1.08}S_{2.2}$
1	40	0	60	Fe_2S_3	45.0	0	55.0	$Fe_{1.09}S_{0.9}$

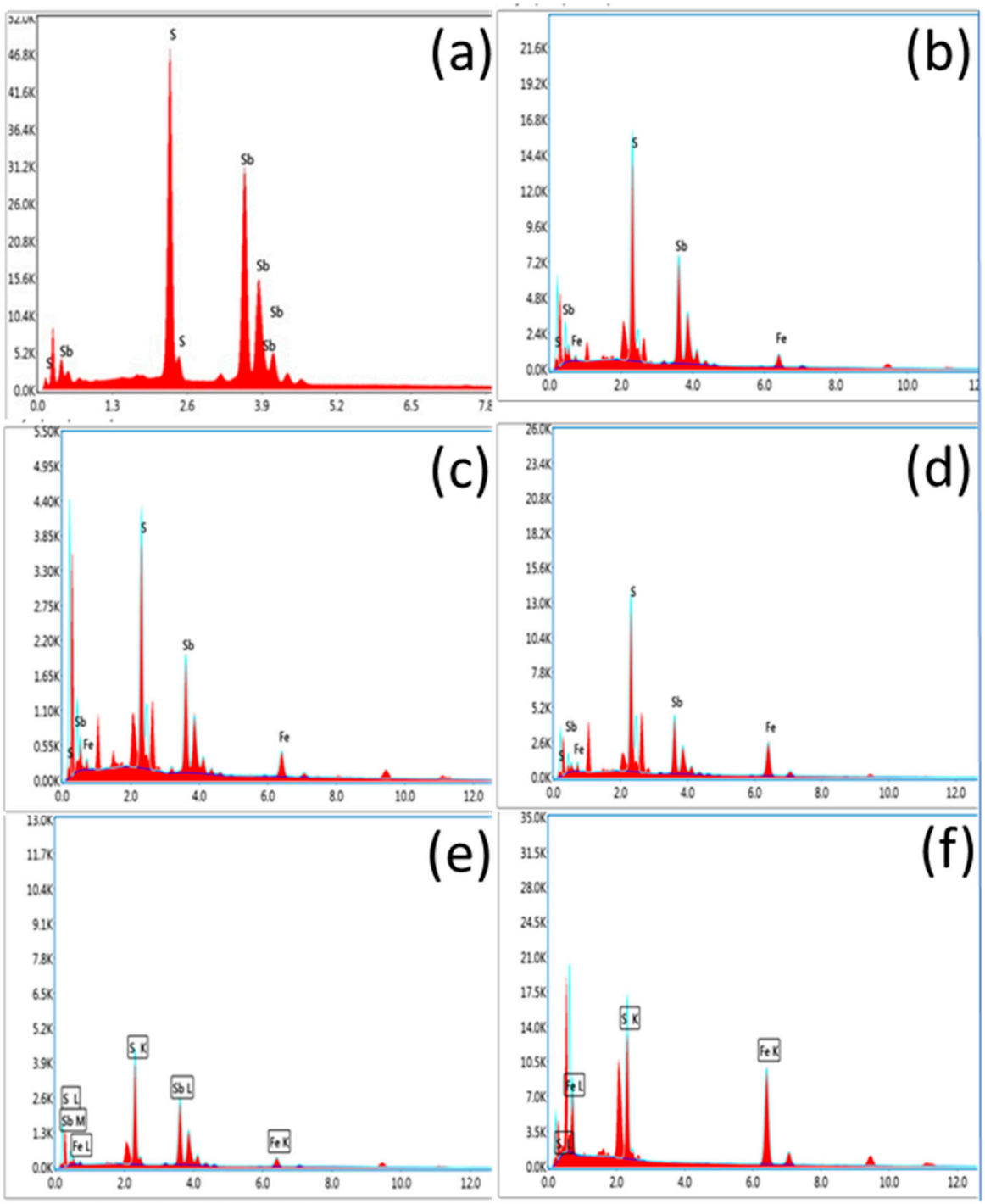

Figure S3. The EDX spectra of $Sb_{2(1-x)}Fe_{2x}S_3$ samples prepared by melt method at 450 °C at various Iron mole fraction (a) x = 0, (b) x = 0.2, (c) x = 0.4, (d) x = 0.6, (e) x = 0.8 and (f) x = 1.

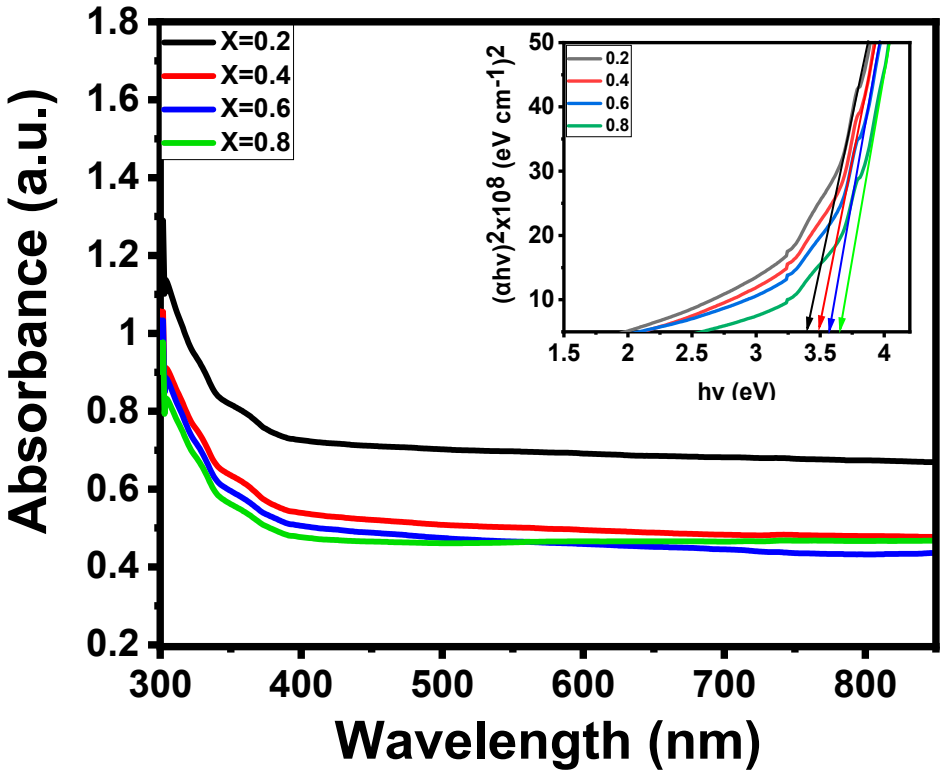

Figure S4. Absorption spectra of $Sb_{2(1-x)}Fe_{2x}S_3$ and inset the tauc plot of $Sb_{2(1-x)}Fe_{2x}S_3$ samples prepared by melt method at 450 °C at various Iron mole fraction x = 0.2, 0.4, 0.6, and 0.8.